J|A|C|S
ARTICLES
Published on Web 04/05/2007

Simultaneous Measurement of Orientational and Spectral Dynamics of Single Molecules in Nanostructured Host−Guest Materials

Christophe Jung,[†] Christian Hellriegel,[†] Barbara Platschek,[†] Dieter Wöhrle,[‡] Thomas Bein,[†] Jens Michaelis,[†] and Christoph Bräuchle*,[†]

Contribution from the Department of Chemistry und Biochemistry, Nanosystems Initiative Munich (NIM) and Center for Nanoscience (CeNS), Ludwig-Maximilians-Universität München, Butenandtstrasse 11, D-81377 München, Germany, and Institut für Organische und Makromolekulare Chemie, Universität Bremen, NW 2, P.O. Box 330440, D-28334 Bremen, Germany

Received November 27, 2006; E-mail: Christoph.braeuchle@cup.uni-muenchen.de

Abstract: Nanostructured host−guest materials are important for various applications in nanoscience, and therefore, a thorough understanding of the dynamics of the guest molecules within the host matrix is needed. To this aim we used single-molecule fluorescence techniques to simultaneously examine the spectral and the orientational behavior of single molecules in nanostructured porous host materials. Two types of host−guest systems have been investigated. First, oxazine-1 dye molecules were fixed rigidly in the channels of microporous $AlPO_4$-5 crystals. Second, it was shown that terrylenediimide (TDI) dye molecules move in the mesoporous network of an uncalcined M41S thin film. In the first sample both spectral fluctuations (∼5 nm) and rare spectral jumps (>10 nm) of the emission maximum were observed. However, the orientation of the emission dipole of the dye molecules remained constant. In contrast, the second system showed orientational dynamics as well as substantially more spectral dynamics. In this system the molecules were found to move between different regions in the host. The typical motion of the TDI molecules in the pores of M41S was not continuous but characterized by jumps between specific sites. Moreover, the spectral and orientational dynamics were correlated and arose directly from the different environments that were being explored by the mobile molecule.

Introduction

Micro- and mesoporous materials play a major role in material science because of the possibility to control their physical and chemical properties. The parameters that can be controlled include pore diameter and pore interconnectivity, as well as the polarity or chemical affinity of the inner surface.[1−3] Furthermore, by incorporating fluorescent dyes into porous solids, one can form so-called host/guest systems that provide an interesting platform for novel technological applications.[4] These applications include micrometer sized dye lasers,[5,6] photoswitchable membranes,[7] and photovoltaic solar cells.[8] The ability to rationally design such systems to obtain materials with improved efficiencies is highly desirable. A complete understanding of the dynamics of the guests within the nanometer sized pores of the host, as well as the host/guest interactions, is therefore urgently needed.

Among the promising porous host materials are crystalline structures, like microporous $AlPO_4$-5 crystals,[9−11] and mesoporous templated silica materials, such as M41S.[1] $AlPO_4$-5 forms large crystals (micrometer-sized) containing homogeneous and one-dimensional pores with a diameter of 0.73 nm. $AlPO_4$-5 crystals allow one to accommodate guest species, for example Xe, and even tightly fitting small dye molecules. Hence, they have attracted much particular attention in fields where molecular recognition is needed, such as catalysis, separations, and chemical sensing. The high regularity of such a structure makes it also interesting for applications in which the stability of the host−guest system is a desirable property. Examples are artificial antennas,[12] ordered materials,[13] nonlinear optical

[†] Ludwig-Maximilians-Universität München.
[‡] Universität Bremen.

(1) Ozin, G. A.; Kuperman, A.; Stein, A. *Angew. Chem., Int. Ed. Engl.* **1989**, *28* (3), 359−376.
(2) Davis, M. E. *Nature* **2002**, *417* (6891), 813−821.
(3) Wirnsberger, G.; Stucky, G. D. *ChemPhysChem* **2000**, *1* (2), 90.
(4) Laeri, F. S. F.; Simon, U.; Wark, M. *Host-Guest-Systems Based on Nanoporous Crystals: Synthesis, Properties and Applications*; Wiley-VCH: Weinheim, Germany, 2003.
(5) Vietze, U.; Krauss, O.; Laeri, F.; Ihlein, G.; Schuth, F.; Limburg, B.; Abraham, M. *Phys. Rev. Lett.* **1998**, *81* (21), 4628−4631.
(6) Braun, I.; Ihlein, G.; Laeri, F.; Nockel, J. U.; Schulz-Ekloff, G.; Schuth, F.; Vietze, U.; Weiss, O.; Wohrle, D. *Appl. Phys. B* **2000**, *70* (3), 335−343.
(7) Weh, K.; Noack, M.; Hoffmann, K.; Schroder, K. P.; Caro, J. *Microporous Mesoporous Mater.* **2002**, *54* (1−2), 15−26.
(8) Gratzel, M. *Nature* **2001**, *414* (6861), 338−344.
(9) Qiu, S. L.; Pang, W. Q.; Kessler, H.; Guth, J. L. *Zeolites* **1989**, *9* (5), 440−444.
(10) Ganschow, M.; Schulz-Ekloff, G.; Wark, M.; Wendschuh-Josties, M.; Wohrle, D. *J. Mater. Chem.* **2001**, *11* (7), 1823−1827.
(11) Wilson, S. T. *Introduction to Zeolite and Science and Practice*; Elsevier: Amsterdam, New York, 1991.
(12) Calzaferri, G.; Huber, S.; Maas, H.; Minkowski, C. *Angew. Chem., Int. Ed.* **2003**, *42* (32), 3732−3758.
(13) Ihlein, G. S.; Ferdi; Krauss, O.; Vietze, U.; Laeri, F. *Adv. Mater.* **1998**, *10* (14), 1117−1119.

10.1021/ja0684850 CCC: $37.00 **© 2007 American Chemical Society**

materials, micrometer-sized dye lasers,[5,6] waveguides,[14,15] and photochromic switches.[7] It is often desirable to accommodate larger species into an ordered porous host, such as biomolecules, large dye molecules, or catalytically active complexes. Sol−gel materials which may accommodate such species are limited by a high intrinsic disorder. In contrast, mesoporous M41S type materials provide pore diameters of sizes larger than about 2 nm up to 20 nm, while retaining an ordered channel system.[16] In addition these amorphous materials show a narrow pore diameter distribution and are available in a variety of morphologies. M41S type materials can be synthesized as films or monoliths of millimeter size. These characteristics make host−guest systems based on these materials extremely interesting for applications such as heterogeneous catalysis,[17] selective sequestration of contaminants,[18] and chromatography.[19]

Characterization methods, such as NMR, IR, UV/vis spectroscopy, electron microscopy, X-ray diffractometry, neutron scattering, etc., have been employed successfully to characterize host−guest materials. However, the behavior of the molecules on the nanometer-scale is both spatially and temporally heterogeneous. A complete characterization of the host−guest material is not possible with these ensemble methods because information about such heterogeneities is lost in the inherent averaging process.

Single-molecule spectroscopy (SMS) is a modern and powerful tool that can elucidate the interactions between an individual molecule and its immediate environment. The experimental data reveal the behavior of each molecule directly, and thus, ensemble averaging is suppressed in SMS measurements.[20−23] The observed spatial and temporal heterogeneities yield a thorough description of the molecule's dynamical behavior as well as of the influence of the environment. SMS methods have been successfully used to characterize the dynamics of individual fluorophores, such as spectral dynamics,[24−27] translational motion,[28] and orientational dynamics.[29−35] Moreover, host−guest materials based on porous solids have been investigated using SMS, revealing for example the influence of the pore structure upon the orientation,[30,36] fluorescence intensity,[37] energy transfer behavior,[38] and diffusion[39,40] of the molecules situated therein. While the measurement of an individual property (e.g., spectrum, orientation, position, etc.) already provides valuable details about the host−guest material, a deeper understanding for the underlying molecular mechanism can be gathered by correlating different properties. For example a longstanding question in SMS studies regards the mechanisms behind the commonly observed fluctuations of emission spectra.[41] This problem can be addressed, for example, by inferring if and how a molecule's spectrum is affected by its orientation in the material.

In this article we present the simultaneous measurement of orientational and spectral dynamics of single dye molecules incorporated into the channels of microporous and mesoporous materials. We monitor simultaneously the full emission spectrum and the in-plane orientation angle of individual emitters in solid porous materials. The results obtained for two types of host−guest material are presented. Oxazine-1 dye molecules incorporated into the channels of microporous $AlPO_4$-5 crystals do not have the freedom to reorient and show limited spectral dynamics. This system represents a static material in which the molecules are entrapped and immobilized in a solid matrix and stands as an example for a static host−guest material, which is desirable for various solid-state optical applications.[4,38] In the second host−guest system, we investigated the movement of terrylenediimide (TDI) dye molecules inside the mesoporous network of an M41S film. TDI molecules are extremely photostable;[42] a single molecule can be studied for several minutes, sometimes hours (compared to only a few seconds of observation time for a typical oxazine molecule). Thus, TDI molecules are ideally suited as reporters for different environments within the nanoporous network. This type of system stands as an example for materials in which dynamics play a fundamental role, as is desirable for sensor and catalysis applications.[43,44] Here, we observe orientational dynamics that are accompanied by spectral dynamics.

Experimental Section

Simultaneous Acquisition of Spectra and Orientation. The experimental setup is based on a confocal ZEISS LSM 410 laser scanning microscope (cf. Figure 1) as described previously.[36] In brief the chromophores are excited with a HeNe laser with $\lambda = 633$ nm. The laser power is measured at the entrance of the microscope objective

(14) Sorek, Y.; Reisfeld, R.; Tenne, R. *Chem. Phys. Lett.* **1994**, *227*, 235.
(15) Yang, L.; Saavedra, S. S.; Armstrong, N. R.; Hayes, J. *Anal. Chem.* **1994**, *66*, 1254.
(16) Ying, J. Y.; Mehnert, C. P.; Wong, M. S. *Angew. Chem., Int. Ed.* **1999**, *38* (1−2), 56−77.
(17) De Vos, D. E.; Dams, M.; Sels, B. F.; Jacobs, P. A. *Chem. Rev.* **2002**, *102* (10), 3615−3640.
(18) Billinge, S. J. L.; McKimmy, E. J.; Shatnawi, M.; Kim, H.; Petkov, V.; Wermeille, D.; Pinnavaia, T. J. *J. Am. Chem. Soc.* **2005**, *127* (23), 8492−8498.
(19) Rebbin, V.; Schmidt, R.; Froba, M. *Angew. Chem., Int. Ed.* **2006**, *45* (31), 5210−5214.
(20) Moerner, W. E. *J. Phys. Chem. B* **2002**, *106* (5), 910−927.
(21) Barkai, E.; Jung, Y. J.; Silbey, R. *Annu. Rev. Phys. Chem.* **2004**, *55*, 457−507.
(22) Kulzer, F.; Orrit, M. *Annu. Rev. Phys. Chem.* **2004**, *55*, 585−611.
(23) Roeffaers, M. B. J. S.; Sels, B. F.; Hiroshi, U.; De Schryver, F. C.; Jacobs, P. A.; De Vos, D. E.; Hofkens, J. *Nature* **2006**, *439*, 572−575.
(24) Lu, H. P.; Xie, X. S. *Nature* **1997**, *385* (6612), 143−146.
(25) Meixner, A. J.; Weber, M. A. *J. Lumin.* **2000**, *86* (3−4), 181−187.
(26) Basche, Th. W. E. M.; Orrit, M.; Wild, U. P. *Single Molecule Optical Detection, Imaging, and Spectroscopy*; Verlag-Chemie: Munich, 1997.
(27) Moerner, W. E. Low-temperature studies in solids. In *Single-Molecule Optical Detection, Imaging and Spectroscopy*; VCH: Weinheim, Cambridge, 1997; pp 1−189.
(28) Schmidt, T.; Schutz, G. J.; Baumgartner, W.; Gruber, H. J.; Schindler, H. *J. Phys. Chem.* **1995**, *99* (49), 17662−17668.
(29) Ha, T.; Enderle, T.; Chemla, D. S.; Selvin, P. R.; Weiss, S. *Phys. Rev. Lett.* **1996**, *77* (19), 3979.
(30) Dickson, R. M. N., D. J.; Tzeng, Yih-Ling; Moerner, W. E. *Science* **1996**, *274* (5289), 966−968.
(31) Hofkens, J.; Verheijen, W.; Shukla, R.; Dehaen, W.; De Schryver, F. C. *Macromolecules* **1998**, *31* (14), 4493−4497.
(32) Bartko, A. P. X.; Kewei; Dickson, R. M. *Phys. Rev. Lett.* **2002**, *89* (2), 026101-1-4.
(33) Piestert, O.; Barsch, H.; Buschmann, V.; Heinlein, T.; Knemeyer, J. P.; Weston, K. D.; Sauer, M. A *Nano Lett.* **2003**, *3* (7), 979−982.
(34) Viteri, C. R.; Gilliland, J. W.; Yip, W. T. *J. Am. Chem. Soc.* **2003**, *125* (7), 1980−1987.
(35) Uji-i, H.; Melnikov, S. M.; Deres, A.; Bergamini, G.; De Schryver, F.; Herrmann, A.; Mullen, K.; Enderlein, J.; Hofkens, J. *Polymer* **2006**, *47* (7), 2511−2518.
(36) Hellriegel, C.; Seebacher, C.; Bräuchle, C.; Ganschow, M. W. *J. Phys. Chem. B* **2003**, *107* (23), 5445−5452.
(37) Higgins, D. A.; Collinson, M. M.; Saroja, G.; Bardo, A. M. *Chem. Mater.* **2002**, *14* (9), 3734−3744.
(38) Megelski, S.; Lieb, A.; Pauchard, M.; Drechsler, A.; Glaus, S.; Debus, C.; Meixner, A. J.; Calzaferri, G. *J. Phys. Chem. B* **2001**, *105* (1), 25−35.
(39) Fu, Y.; Ye, F. M.; Sanders, W. G.; Collinson, M. M.; Higgins, D. A. *J. Phys. Chem. B* **2006**, *110* (18), 9164−9170.
(40) Hellriegel, C.; Kirstein, J.; Bräuchle, C. *New J. Phys.* **2005**, *7* (23), 1−14.
(41) Stracke, F. B.; Christian; Becker, S.; Müllen, K.; Meixner, A. J. *Chem. Phys.* **2004**, *300* (1−3), 153−164.
(42) Jung, C.; Muller, B. K.; Lamb, D. C.; Nolde, F.; Mullen, K.; Brauchle, C. *J. Am. Chem. Soc.* **2006**, *128* (15), 5283−5291.
(43) Konya, Z.; Puntes, V. F.; Kiricsi, I.; Zhu, J.; Alivisatos, P.; Somorjai, G. A. *Catal. Lett.* **2002**, *81* (3−4), 137−140.
(44) Konya, Z.; Puntes, V. F.; Kiricsi, I.; Zhu, J.; Ager, J. W.; Ko, M. K.; Frei, H.; Alivisatos, P.; Somorjai, G. A. *Chem. Mater.* **2003**, *15* (6), 1242−1248.

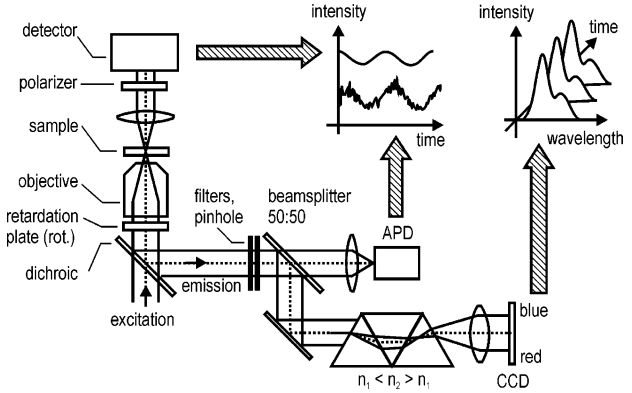

Figure 1. Experimental setup for the simultaneous measurement of orientations and spectra of single molecules based on a confocal microscope.

(1.4 NA Zeiss 63×, oil immersion objectives) used for illumination and collection of fluorescence. The polarization of the excitation light is modulated using a $\lambda/2$ retardation plate rotating continuously at ~3 Hz. The polarization is monitored in transmission using a conventional polarizer−detector unit. The red-shifted fluorescence light from the fluorophores in the sample is separated from the excitation light with a combination of a dichroic (Q640LP, AHF Analyzetechnik), notch (633 nm notch, Kaiser), and long-pass (HQ720/150, AHF Analyzetechnik) filters. The fluorescence light then passes a 50:50 beam-splitter and is routed to two detectors.

The first detector, an avalanche photodiode, APD (EG&G SPCM-AQ 141), records the modulated fluorescence intensity as the polarization plane of the excitation light is constantly being rotated. These data are evaluated against the polarization of the incident light and yield the in-plane orientation angle of the fluorescence signal.

The second detector, a prism-CCD spectrometer (Princeton Instruments, EEV 1300/100-EMB-chip), records the emission spectra. Data acquisition is synchronized with the rotation of the $\lambda/2$ plate so that one spectrum is acquired for each 180° revolution of the excitation polarization (yielding an integration time of ~300 ms). Compared to grating spectrometers, the prism used in this setup has a superior transmission efficiency (~80%) allowing us to acquire well-resolved spectra in a comparatively short time interval.

To acquire a set of data for an individual molecule, that is, the polarization-dependent intensity traces and sequences of spectra, we proceed as follows: In the first step an image of the sample is acquired corresponding to an area of approximately 25 × 25 μm. At ultralow concentration of the fluorophore within the sample, it is possible to observe diffraction limited fluorescence patterns in the images which show the typical behavior for individual fluorophores, i.e., intermittent emission and abrupt photobleaching. The confocal volume of the microscope, which is an ellipsoid of roughly 300 nm in the focal plane and 900 nm along the optical axis, can then be centered on such a fluorescent spot. One can then record the polarization dependent fluorescence intensity trace, as well as a sequence of fluorescence spectra of the single molecule.

Orientation Determination. The polarization dependent data obtained with our setup consists of two modulated signals that follow a cosine-square law. The first signal, acquired from the transmitted laser light, defines the orientation of the excitation polarization and is used as a reference. The second signal, the single-molecule fluorescence intensity, is modulated depending on the alignment of the fluorophore's transition dipole moment with respect to the excitation polarization. For the analysis the data are divided into segments of approximately 300 ms (corresponding to one 180° revolution of the polarization plane). These segments are subsequently analyzed using the following equations:

$$I_T(t) = A_T \cos^2(\omega t + \phi_T) + c_T \quad (1)$$

$$I_F(t) = A_F \cos^2(\omega t + \phi_F) + c_F \quad (2)$$

Here I_T is the transmission intensity and I_F the fluorescence intensity, $A_{T,F}$ the amplitude of the modulations, ω the rotation frequency, $\phi_{T,F}$ the phases, and $c_{T,F}$ the offsets, e.g., which are caused by unspecific background. Note that these two equations share the frequency ω as a common parameter. The in-plane orientation of the molecule with respect to the reference in this segment is then

$$\Phi = \phi_T - \phi_F \quad (3)$$

The operation is repeated by shifting the segment by one, two, three, etc., data points. In this way it is possible to obtain the molecule's orientation Φ as a function of time. In the following we will refer to $\Phi(t)$ as the angular trajectory. The error in Φ, given by the standard deviation from the fitting procedure, varies with the quality of the data, e.g., signal-to-noise, and is typically in the range between 2 and 5°.

Analysis of Spectral Dynamics. Sequences of single-molecule spectra are acquired simultaneously with the modulated intensity traces. All spectra are calibrated to compensate for the nonlinear dispersion curve of the prism and wavelength dependencies of the setup used. Additional unspecific fluorescence from the sample is recorded for every sequence of spectra after photobleaching of the observed molecule and subtracted from the data. The spectra of oxazine-1 and TDI show one pronounced main band followed by a broad vibronic shoulder and can be fitted using a double Gaussian model:

$$I(\lambda) = A_m \exp[-(\lambda - \lambda_m)^2/2w_m^2] + A_s \exp[-(\lambda - \lambda_s)^2/2w_s^2] \quad (4)$$

In this equation $A_{m,s}$ are the amplitudes and $\lambda_{m,s}$ the central wavelengths of the main band and the side pear, respectively. Parameters $w_{m,s}$ are the waist of the respective Gaussian. The result of the fitting procedure is a sequence of spectral fit parameters, i.e., central wavelengths, amplitudes, and widths, which describe the respective spectrum. The main parameter used in this article is the central wavelength of the main band, λ_m, and its variations with time. We will refer to $\lambda_m(t)$ as the spectral trajectory. The experimental error for the estimation of the central wavelength varies with the signal-to-noise ratio and lies typically between 0.5 and 2 nm (standard deviation of Gaussian fit).

Synthesis of the Oxazine-1/$AlPO_4$-5 System. Oxazine-1-loaded $AlPO_4$-5 crystals were prepared by the microwave-assisted hydrothermal synthesis as described previously.[10,36] The crystal structure of the samples was determined by X-ray diffraction (Philips PW-1050 X'Change, Cu-Ka1, Bragg−Brentano geometry, secondary monochromator), and its morphology was visualized by scanning electron microscopy (ISI-100B, 15 kV; data not shown). The crystal structure and the morphology of $AlPO_4$-5 were not affected by the inclusion of the dye molecules. The $AlPO_4$-5 crystals appeared as micrometer-sized hexagonal barrels with bulges on both ends (size ~8 × 5 μm). The crystals with low loading contained dye concentrations of $\sim 10^{-10}$ mol g^{-1}. The one-dimensional pores were perpendicular to the hexagonal sections of the crystals, that is, parallel to the long axis of the barrel.

Synthesis of the TDI/M41S System. The hexagonal M41S silica films were synthesized onto glass coverslips via evaporation-induced self-assembly (EISA).[45] Samples were prepared by spin-coating onto glass microscopy coverslips. To avoid unspecific fluorescence from impurities, the glass substrate was cleaned before the synthesis procedure using a 1% Hellmanex solution (Hellma) in an ultrasonic bath (2 min at 60 °C) and subsequent rinsing with deionized and UV irradiated water. A 10 mmol (2.08 g) amount of tetraethoxysilane in 534 mmol (7.9 g) of ethanol was prehydrolyzed at 60 °C for 1 h under acidic catalysis (using 3 g of 0.2 M hydrochloric acid and 1.8 g of water). A 1.75 mmol (638 mg) amount of cetylhexyltrimethylammo-

(45) Brinker, C. J. L.; Yunfeng; Sellinger, A.; Hongyou, F. *Adv. Mater.* **1999**, *11* (7), 579−585.

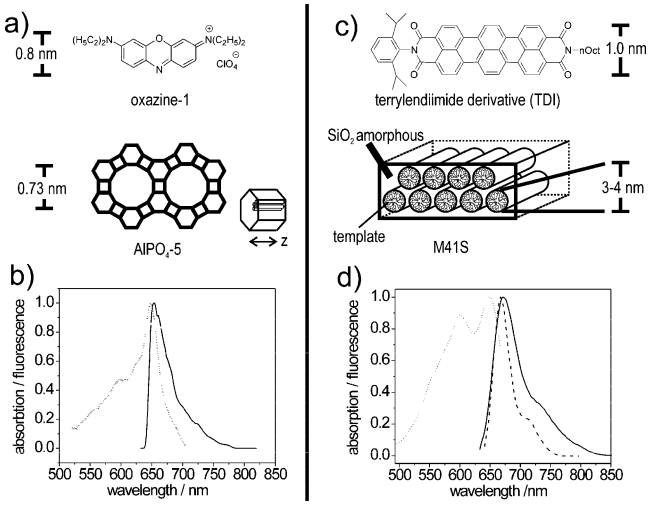

Figure 2. Chemical structures, sizes of guests and hosts, and spectra of the investigated samples. (a) Oxazine-1 (width 0.8 nm) and the unidimensional channels of $AlPO_4$-5 (diameter 0.73 nm) viewed from the front. The small scheme on the lower right shows the crystal habitus and the direction of the pores. (b) Absorption (dotted line) and emission (solide line) spectra of oxazine-1 in high loading (10^{-8} mol g^{-1}) in $AlPO_4$-5 crystals. (c) Terrylenediimide derivative (TDI, 1.0 nm in width) and the hexagonally ordered channels (diameter 3−4 nm) of the template-filled M41S structure. (d) Absorption (dotted line) and emission (solid line) spectra of TDI in ethanol and emission spectrum of TDI in high concentration (10^{-5} mmol/L) in a M41S film (dashed line).

niumbromide (CTAB), the structure directing agent, in 1068 mmol (15.8 g) of ethanol was added. Furthermore, TDI was added to the solution at ultralow concentration (10^{-9} mol/L). This precursor solution was then spin-coated onto a coverslip. The fast evaporation of the volatile solvent induces the micellization of the template and self-organization of the silica species simultaneously with the condensation of the silica. This procedure results in structured silica films with a thickness of about 200 nm (determined by ellipsometry). The films are left uncalcined; that is, the template in the pores of the M41S films acts as a solvent. Since residual water remaining within the pores might influence the dynamics, we have placed the sample at constant relative humidity of ∼40% during all the measurements.

The structure of the pores in the film was determined using a Scintag XDS 2000 powder diffractometer in a $\theta/2\theta$ Bragg−Brentano scattering geometry (data not shown). The mesostructured films exhibit 2D-hexagonal order; that is, the amorphous silica surrounding the CTAB−micelles forms hexagonally packed cylindrical pores (see Figure 2b). These pores lie parallel to the substrate surface and are organized in 100−500 nm sized crystallike domains. In the plane of the substrate these domains are randomly rotated against each other.[46]

Results and Discussion

The molecules investigated are incorporated as guests into the pores of molecular sieves. The two systems that have been studied are depicted in Figure 2. In the first system oxazine-1 molecules are encapsulated into the unidimensional channels of $AlPO_4$-5 crystals (a zeotype structure). In this case the width of the molecules (∼0.8 nm) and the diameter of the pores (0.73 nm) are comparable (Figure 2a). The molecules fit tightly into the channel structure, and we do not expect the molecules to reorient, or to show any mobility at all, in accordance with previous studies.[36] Absorption and emission spectra for a highly loaded crystal (∼10^{-8} mol g^{-1}) are shown in Figure 2b.

(46) Klotz, M.; Albouy, P. A.; Ayral, A.; Menager, C.; Grosso, D.; Van der Lee, A.; Cabuil, V.; Babonneau, F.; Guizard, C. *Chem. Mater.* **2000**, *12* (6), 1721−1728.

In the second system we chose the relevant sizes of host and guest to allow for more orientational dynamics. Here, terrylenediimide (TDI) molecules are incorporated into the pores of an uncalcined M41S film, a templated mesoporous silica material (cf. Figure 2c). Absorption and emission spectra for higher concentration (∼10^{-8} mol L^{-1}) are shown in Figure 2d. TDI molecules are extremely photostable;[42] a single molecule can be studied for several minutes, sometimes hours (compared to only a few seconds of observation time for a typical oxayzine molecule). Thus, TDI molecules are ideally suited as reporters for different environments within the nanoporous network.

Oxazine-1/$AlPO_4$-5 System. A typical fluorescence microscopy cross section through an $AlPO_4$-5 crystal containing oxazine-1 molecules is shown in Figure 3a. The approximate boundary of the crystal in this image is obtained from transmission images. The individual molecules are visible as diffraction-limited fluorescence spots. The confocal volume can be placed on one of the corresponding positions to acquire data from an immobilized single molecule. During this acquisition the excitation polarization is rotated continuously. Excerpts from the data sets for a single oxazine-1 molecule in $AlPO_4$-5, that is, the polarization-dependent intensity trace and the sequence of spectra, are shown in Figure 3b,c.

The curves in Figure 3b show the typical cosine-square modulation for the transmitted light (top graph) and a single oxazine-1 molecule (middle graph). The data can be fitted with eqs 1 and 2, respectively. The orientation of the molecule remains constant with a value of 143 ± 2°. The angular distribution of all molecules is broad and roughly aligned with the main axis of the crystal.[36] Altogether 60 molecules in 5 different crystals were measured, and all molecules remained with a fixed orientation during the measurement. This confirms our expectation that the tight fit of oxazine-1 molecules in $AlPO_4$-5 results in immobile molecules that do not have any freedom to move or to rotate.

Simultaneously with the polarization data, we recorded fluorescence spectra and observed spectral dynamics. With these data we can differentiate between fast spectral fluctuations and rare spectral jumps. In the first case, the spectral position of the emission maximum fluctuates continuously around a mean value. The amplitude of these fluctuations varies and is typically in a range 2−8 nm. In contrast, *spectral jumps* occur abruptly as isolated events and the jump is typically larger in magnitude than the *spectral fluctuations*. An example showing such a pronounced spectral jump is shown in Figure 3c. The two spectra were taken consecutively and correspond to the time segments A and B indicated in the intensity trace in Figure 3b. The spectra before the jump resemble spectrum A, and the ones after the spectral jump event resemble B (data not shown). An intermediate and broadened spectrum is not observed on going from spectrum A to spectrum B. This is a clear indication that the jump itself takes place on a time scale well below our temporal resolution (∼300 ms)

The data analysis of the modulated intensity trace and sequence of spectra give $\Phi(t)$, the angular trajectory, and $\lambda_m(t)$, the spectral trajectory (cf. Orientation Determination section). The graphs in Figure 3d,e show the corresponding data for the molecule displaying the spectral jump mentioned above and for another, more representative oxazine-1 molecule in an $AlPO_4$-5 crystal. In the first case we determined that the emission

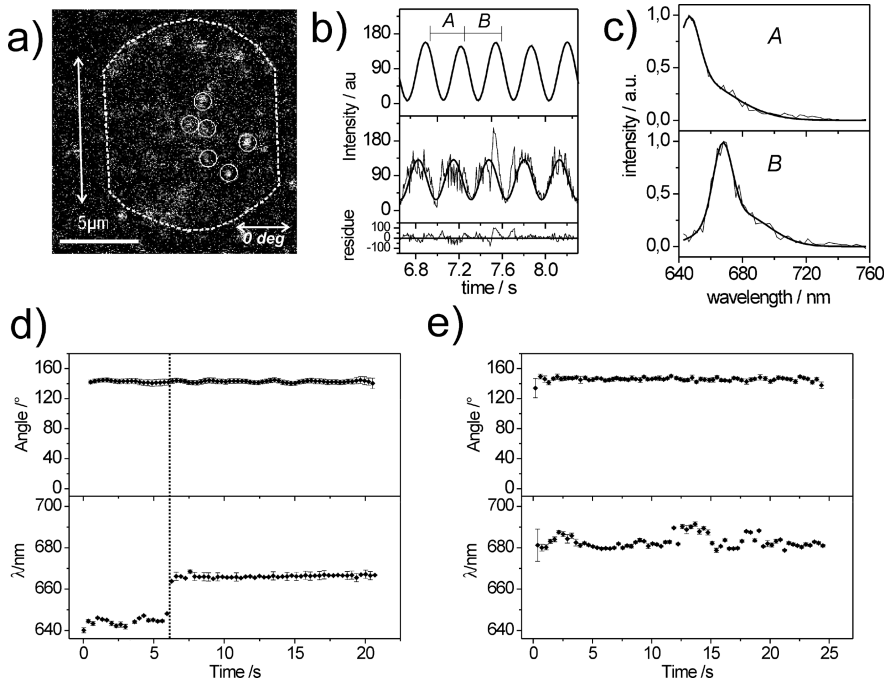

Figure 3. Simultaneous measurement of orientation and spectra of single oxazine-1 molecules in $AlPO_4$-5 in loadings of 10^{-10} mol g^{-1}. (a) Confocal cross section through an $AlPO_4$-5 crystal showing single molecules as diffraction-limited fluorescence spots. The outline of the crystal shape (dotted line) and the pore orientation (arrow) are inferred from transmission images. (b) Polarization-dependent intensity trace for transmitted excitation light (upper graph) and single-molecule fluorescence (middle graph). The solid curve is the fit of eq 1 to the data. The lower graph shows the residuals of the fit. (c) Two consecutive spectra (with fits) corresponding to the time segments A and B (indicated in (b) showing a pronounced spectral jump of 26 nm. (d) Complete angular and spectral trajectories corresponding to the graphs in (b) and (c). Error bars in (d) and (e) denote the standard deviation of the fit. (e) Angular and spectral trajectories for another oxazine-1 molecule showing the most common case encountered in this system.

maximum makes a jump of 26 nm to larger wavelengths at approximately 7.5 s in Figure 3d. However, before and after the jump the orientation remains constant. Upon closer inspection of the polarization dependent data shown in Figure 3b, it is possible to note a burst in the intensity trace at the time when the spectral jump occurred. This jump might indicate a short-lived change in the environment. Spectral jumps of this magnitude have been observed rarely in this system; 3 out of 60 molecules showed a single spectral jump. On a cumulative time scale, this corresponds to about 1 jump/3 min of observation time. The second set of data (Figure 3e) is more representative for the oxazine-1/$AlPO_4$-5 systems. The orientation of the molecule also remains constant (149 $\pm$ 5°) while the spectra fluctuate rapidly around a mean value of 685 nm in a range 2−8 nm.

The encountered spectral dynamics are a consequence of the changes of the underlying electronic energy levels. It has been suggested that they can have *intrinsic* or *extrinsic* origins.[41] Different interconvertible structural conformations of a chromophore producing spectral shifts are an example for intrinsic factors.[25] On the other hand, the interactions between the electronic states of the chromophore with its immediate environment can lead to spectral fluctuations of extrinsic origin. This is the case if the immediate vicinity of the molecule is subject to dynamical changes or if the molecule moves to different environments in the host. Possible causes for the fluctuations in the molecule's direct vicinity include the motion of small charged molecules in neighboring channels or conformational changes in the host structure near the site at which the fluorescent molecule is located.

The absence of detectable orientational dynamics confirms that in this system oxazine-1 is tightly confined in the pores of $AlPO_4$-5. On the other hand, spectral dynamics are clearly visible and confined to a range of typically 3−5 nm. In a few isolated cases pronounced spectral jumps (up to 26 nm) have been observed. These fluctuations reflect dynamical changes in the environment around the molecule since the molecule is not moving to different sites in the crystal. Possible causes for such small and rapid fluctuations can be fluctuations in the $AlPO_4$-5 structure[47] or interactions with coadsorbed species (ions, water, template) which are comparatively free to diffuse in the pores of the material.[48] The large spectral jumps must result from more pronounced and rarely occurring events. Possible reasons for these events could be the direct interaction with a coadsorbed species in the same channel or (counter-) ions changing between comparatively stable adsorption sites in neighboring pores interacting via the Stark effect. Whereas in this section we have observed the behavior of individual dye molecules in a static material, we turn in the next section to a dye−pore system in which the dye molecules have more space to undergo orientational dynamics.

TDI/M41S System. The orientational and spectral dynamics in the TDI/M41S system are expected to be more complex than in the oxazine-1/$AlPO_4$-5 system because of the larger mobility of the molecules in this matrix. The TDI molecules are smaller (~2.5 nm in length, ~1.0 nm in diameter) than the M41S pore diameter (3−4 nm). However, it is important to recall here that the structured channels in the otherwise amorphous SiO_2 body are left uncalcined; that is, the pores in which TDI molecules are situated are filled with the micellar template CTAB used for the synthesis. Translational diffusion occurs in this medium and allows the molecules to explore different environments.

(47) Bordat, P.; Brown, R. *J. Chem. Phys.* **2002**, *116* (1), 229−236.
(48) Kaerger, J. *Adsorption* **2003**, *9* (29), 35.

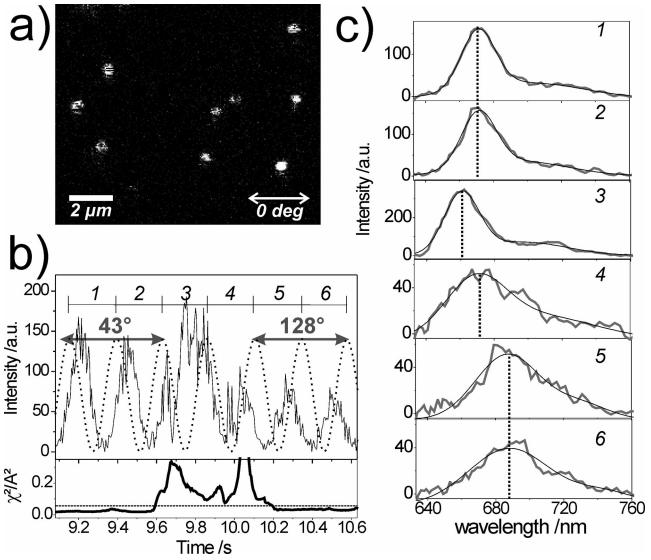

Figure 4. Images and data sets for single TDI molecules in an M41S film. (a) Fluorescence image showing diffraction-limited fluorescence spots of individual TDI molecules in a M41S film. (b) Polarization-dependent fluorescence intensity trace (full line) and transmitted excitation light (dotted line) curves showing orientational dynamic of an individual TDI molecule. The lower graph shows the normalized χ^2 which is used as a criterion (threshold given by dotted line) to assign an orientation to a time segment. For details see text. (c) Sequence of spectra corresponding to the segments indicated in (b). The dashed line indicates the center position of the fit to the spectrum.

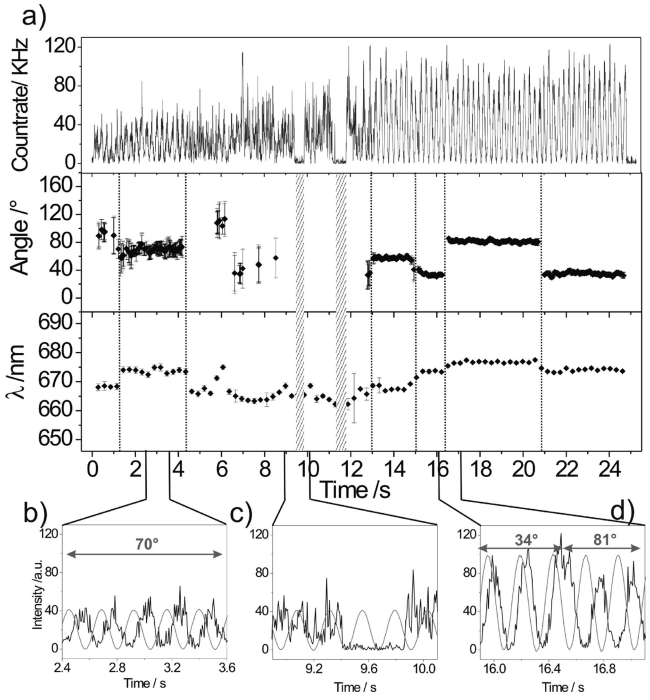

Figure 5. Orientational behavior of TDI in a M41S film. (a) The upper panel shows the polarization-dependent fluorescence trace. The middle and lower panels give the angular and spectral trajectory after data analysis. (b−d) Excerpts from the curve in (a). The continuous thin line corresponds to the excitation polarization. (b) A stable orientation of ∼70° over a period of seconds. (c) Segment where no preferred orientation could be assigned and blinking event occurred. (d) Time window with distinct jump from 34 to 81°.

During this movement the molecule is free to change its orientation. Translational diffusion, however, is slow enough to ensure that a molecule remains within the detection volume of the confocal microscope for several minutes.

A typical data set consisting of images and orientational and spectral data for TDI in M41S is shown in Figure 4. The data were obtained in the same manner as described for the oxazine/$AlPO_4$-5 system. For clarity, we divide the discussion into three parts. We will first present the different types of orientational dynamics we encountered in this system and will then, in the second part, proceed to correlate these data with the spectral dynamics. In the last part we give a global statistical description using all observed dynamics for 72 investigated molecules.

Orientational Dynamics. TDI in M41S shows pronounced orientational dynamics. A typical example is depicted in Figure 4b. In this excerpt from a longer intensity trace, the molecule starts with a well-defined orientation (of 43 ± 2°) and remains oriented for about 0.6 s. Then, in the time interval between 9.6 and 10.1 s, it is not possible to determine a stable orientation. This is a clear indication that in this period the molecule is undergoing orientational dynamics that are below our temporal resolution of 300 ms. Then, at 10.1 s, the molecule finds a new stable orientation, at a different angle (128 ± 3°). It is interesting to note that the intensities before and after the reorientation period are not equal. This is most likely caused by different (out-of-plane) orientations of the molecule with respect to the optical axis of the experiment. Other possibilities for a change in fluorescence signal are the lateral diffusion out of or into the center of the confocal volume or the fact that the molecules may explore different environments which may affect the fluorescence intensity.[49]

This type of orientational dynamics, that is, a molecule starting with one well-defined orientation, undergoing some form of movement in the porous matrix and ending at a new stable orientation, is the most commonly observed case in the TDI/M41S system. We interpret this as a molecule moving between different adsorption sites in the material. The nature of these adsorption sites is currently not very well understood; possible interactions include direct contact with silica walls and electrostatic interactions with the cationic template as well as interactions at defect sites. The binding to the adsorption site is revealed by the molecule's fixed orientation for a certain period of time. The duration of this period relates to the strength with which the molecule interacts with the site. We will therefore in the following discussion use the adsorption duration as a measure for the interaction strength.

To describe the orientational behavior in more detail, we now turn to another single-molecule example depicted in Figure 5. The polarization-dependent intensity trace is shown in the upper panel of Figure 5a. The middle graph shows the extracted angular trajectory $\Phi(t)$. Only those data points are displayed for which a well-defined orientation can be determined; i.e., the orientation is constant during at least one period of the polarization modulation. The omitted points correspond to segments during which the molecule underwent rapid reorientations, so that no stable orientations could be determined. The two hatched segments correspond to so-called blinking events, where the molecule rests in a dark state.

The time scales on which the orientational dynamics occur range from below our temporal resolution, of 300 ms, to tens of seconds. To illustrate this we turn to a few exemplary time

(49) Bardo, A. M.; Collinson, M. M.; Higgins, D. A. *Chem. Mater.* **2001**, *13* (8), 2713−2721.

segments in Figure 5b−d which are taken from the complete trace of Figure 5a. The segment in Figure 5b shows that orientations may remain stable on a time scale of seconds. This indicates that strong adsorption sites in the material are accessible to the moving molecule.

The graph in Figure 5c is an excerpt from the period between 4.2 and 13 s and shows a different characteristic behavior. Here, the molecule undergoes rapid orientational dynamics for a period of seconds. This indicates the presence of regions in which the interactions between the molecule and the matrix are weaker. In this region, the molecule is continuously tumbling between different environments.

In Figure 5d an abrupt reorientation is shown, in contrast to the more commonly observed phenomenon, where a period of high dynamics is found in between two adsorption events, described above. In this example, the movement itself is much faster than our resolution limit. The molecule starts with an orientation of 34 ± 2° and jumps to 81 ± 2°. Later in the trajectory (at about 21 s), as can be seen in the middle graph of Figure 5a, the molecule switches back abruptly to the same angle of 34°. This particular case shows a molecule switching abruptly back and forth between preferential orientations. This switching is likely caused by sites where two stable positions, i.e., two minima in the effective potential, are present. This is a clear example for a situation where additional information about the molecule, e.g., its emission spectrum, could help to distinguish between two plausible explanations.

The individual molecules explore various environments in which the time scale of the orientational dynamics varies dramatically. In one extreme case a molecule may stay at a specific well-defined orientation, at a strong adsorption site for many seconds—indicated by a constant orientation angle. On the other hand a molecule can be found to undergo fast orientational dynamics that last for a period of several seconds, if it is within a region in which the host−guest interactions are comparatively weak and the molecule is able to sample different areas. Altogether these behaviors reflect the heterogeneous structure of the environment that is explored by the molecule.

In the next section we include the spectral data to address the question how the travel to different adsorption sites can affect the spectral properties of the fluorescent molecules.

Combined Spectral and Orientational Dynamics. To gain a more detailed understanding about the nature of the observed adsorption sites, we simultaneously record the fluorescence spectra of the individual dye molecules. Taken by themselves, the spectral dynamics in the TDI/M41S system are similar to those observed in the oxazine-1/$AlPO_4$-5 system; that is, we observe fast changes of the emission spectra on a 2−30 nm scale. Likewise, it is possible to differentiate between *spectral fluctuations* (occurring continuously and fast) and *spectral jumps* (isolated events, larger in magnitude and less frequent). Such large spectral jumps, spanning a range of 27 nm, are shown in Figure 4c. These spectra correspond to the numbered segments of the fluorescence intensity trace shown in Figure 4b. The emission maximum of the spectrum remains nearly constant (at around 685 nm) in the first two spectra. During that time the polarization analysis yields a stable angle of 43°. The emission maximum changes in the next two periods (spectra 3 and 4) until a new stable position is found in spectrum 5 and in the subsequent segments with an emission maximum at 688 nm. Here, the molecule is found at a fixed orientation of 128°.

Upon closer inspection of the periods during which the spectral jumps occur, we note that spectrum 3 is narrower than spectrum 4. This indicates that the interaction with the environment leading to spectrum 3 does not cause large fluctuations. At the same time, the polarization signal of the molecule does not allow one to find a stable orientation. This may be so if the molecule stayed at a preferential orientation for a time just below our temporal resolution. We therefore determined the orientation in segment 3 using only half a modulation period and obtain an angle of 105°, however, with a large error of 20°. Altogether, this information suggests that the molecule first switches rapidly between adsorption sites on going from segment 2 to 3 and then undergoes even faster spectral and orientational dynamics in segment 4.

The correlation between orientational and spectral dynamics is shown on a larger time scale in the lower panel of Figure 5a for another single molecule. For clarity, we do not display the complete spectrum but show the spectral position of the emission maximum, $\lambda_m(t)$. First, we note the presence of periods during which the maximum of the emission spectrum remains at a constant value, thus yielding a plateau in the time trace. Each plateau in the spectral trajectory can be assigned to a plateau in the orientational trajectory, in the same time range. Spectral and orientational jumps can be seen in the whole time trajectory. These jumps are usually correlated neither in size nor in direction. However, sometimes we observe reversible jumps. An example is seen in the three last plateaus that correspond to two distinguishable spectral positions (674, 677 nm) and can be assigned to the two angular positions (34, 81°), as discussed above. This further strengthens our argument that in these last periods (from 14.8 to 24.5 s) we are studying a molecule that is switching back and forth between two well-defined adsorption sites.

The many details obtained by our method reveal some more characteristic effects that are worth mentioning. To illustrate these, we show two more trajectories in Figure 6a,b. Due to the high photostability of TDI it is possible to observe the behavior of a single molecule on a time scale of minutes. The behavior is extremely heterogeneous. In the first part of the trajectory in Figure 6a (until 85 s) the plateaus extend over a long period of time. Here, the molecule is situated in a region where the interactions with the material are strong. Then, in the time segment between 85 and 150 s the molecule undergoes a long period of orientational and spectral dynamics. Here, the molecule has moved into an environment where the interactions are weaker. This allows the molecule to explore a more extensive set of adsorption sites. In the last part of the trajectory, i.e., after 150 s in the trace, the interactions become stronger again.

A special case can be seen at about 8 s in the trajectory. The molecule undergoes a large orientational jump from the stable orientation at 150° to a stable orientation at 82°. The corresponding spectra, however, are peaked at identical wavelengths. While the orientational jumps manifest that the molecule changes its position, the similarity of the spectra suggests that the molecule finds two environments which are similar in terms of host−guest interaction.

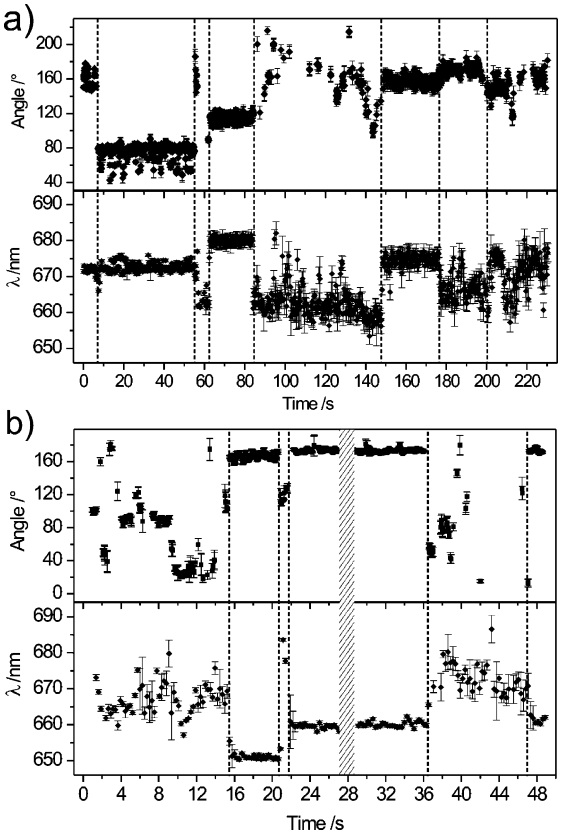

Figure 6. Angular and spectral trajectories for two TDI molecules in M41S. The trajectories in (a) and in (b) show special cases of orientational and spectral dynamics discussed in the text. The error bars denote the standard deviation of the fits.

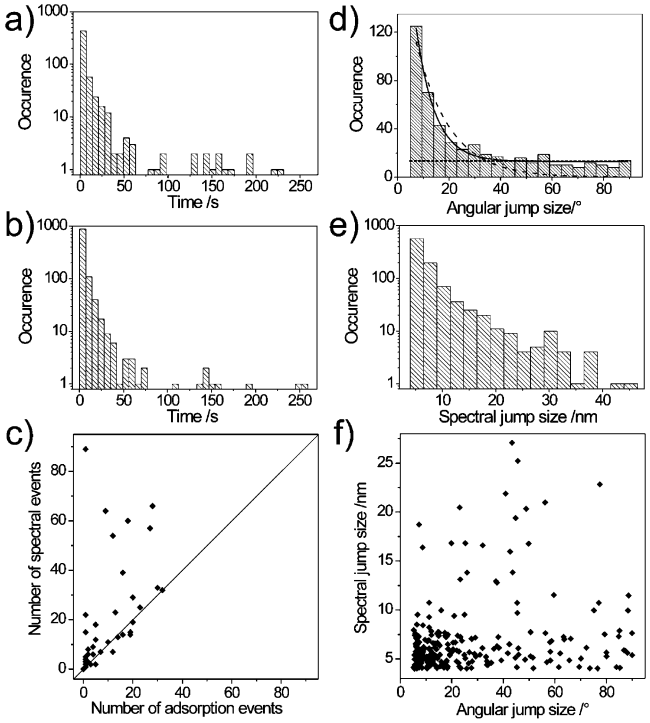

Figure 7. Global correlation between adsorption and spectral residence times of TDI molecules in M41S. (a) Histogram showing the distribution of adsorption (angular) times. (b) Histogram of spectral residence times. (c) Cross-correlation between number of spectral and adsorption events per molecule. (d) Histogram showing the distribution of angular jumps sizes. A single-exponential fit to the data (dashed line) does not agree with the observed distribution. A single-exponential fit (solid line) in combination with an offset (dotted line) describes the data much better (see text for details). (e) Histogram of the spectral jump size. (f) Cross-correlation between magnitudes of concomitant angular and spectral jumps.

The second trajectory displayed in Figure 6b shows the data from a different molecule which displays similar spectral and orientational dynamics during large parts of the trajectory. Moreover, a rare case is also observed where the molecule visits a particular adsorption site twice, interrupted by a long time interval between the events. The adsorption site yields the molecule at a stable orientation (175 ± 2°) between 22 and 36 s. This period is followed by a long interval of strong orientational and spectral dynamics from 36 to 47 s. After this period both the angle and the emission maximum return to the original values. In this case, the molecule is either returning to the same adsorption site or—by coincidence—finds another adsorption site with the same angle and with a very similar environment.

In conclusion, the juxtaposition of orientational and spectral behaviors gives a more complete picture of the system investigated. The observed strong correlation between spectral and orientational jumps shows that the spectral fluctuations are a direct consequence of the host−guest interactions.[34,50] Therefore, it is possible to use an individual molecule as a reporter for its immediate nanoenvironment. Furthermore, from our data we can conclude that the interaction between the molecule and an adsorption site in the material is quite specific. That is, a distinct host−guest interaction produces its own characteristic spectrum. The spectral fluctuations are comparatively small when a molecule is fixed at an adsorption site. Moreover, molecules are exploring different adsorption sites as indicated by simultaneous occurrence of orientational and spectral jumps. The part of the trajectory during which a molecule moves is characterized by rapid reorientations that cannot be assigned to a specific angle, as well as by strong fluctuations in the spectral trajectory. The magnitude of the fluctuations during this period is significantly larger than the magnitude of the fluctuations when the molecule is found to have a constant orientation. A likely cause for these large fluctuations is the rapid succession of different environments explored by the molecule during its motion. Thus, a single molecule can explore nanometer scale heterogeneities in its surroundings. The recorded data, the orientation and emission spectrum, are clear footprints of these heterogeneities.

Statistical Analysis of All Traces. While the high sensitivity of SMS reveals many details of host−guest interactions—in fact, every single trace is unique—it is also useful to compare the behavior of all molecules by computing histograms and correlations. The following questions will be addressed: (a) What is the typical time a molecule spends at a specific orientation? (b) What is the typical time a molecule is found with a specific spectrum? (c) Can the distribution of spectral and orientational jumps be characterized? (d) Do all spectral jumps occur simultaneously with orientational jumps?

We have computed histograms of orientational and spectral residence times (the lengths of the plateaus in the graphs) from 72 trajectories. The result is displayed in Figure 7a. The typical time a molecule spends at a specific orientation is computed

(50) Mahurin, S. M.; Dai, S.; Barnes, M. D. *J. Phys. Chem. B* **2003**, *107* (48), 13336−13340.

from the angular trajectory using a threshold criterion for the variation in the angle from data point to data point. The time a molecule spends at one orientation ends with an orientational jump exceeding a threshold value of 5° (this value is about two times the typical experimental error). The distribution of residence times is shown in Figure 7a. It does not follow a monoexponential model; this indicates that there are different effects leading to the distribution. These effects include the kinetics of adsorption and desorption of a dye molecule to specific sites of the matrix and influence of template dynamics and of other species present in the porous network To obtain a characteristic time we determine the median of the distribution, which for this system is 2.3 s.

Similarly, we obtained the distribution of spectral residence times by applying a threshold value of 4 nm (twice the typical experimental error). Likewise, the distribution (Figure 7b) does not follow a monoexponential model. The median, used to describe a characteristic time between jumps is 2.2 s. Usually, diffusion of molecules occurs on much faster time scales. Therefore, in this system albeit diffusion is possible it is greatly hindered by strong adsorption sites and the presence of the template.

To verify quantitatively to what extent angular and spectral jumps are correlated, we plot the number of angular jumps versus the number of spectral jumps per molecule in Figure 7c. If the orientational and spectral jumps were absolutely correlated all data points would be located on the $y = x$ diagonal. The graph shows, however, that while spectral jumps correlate with orientational jumps, they also occur in the absence of orientational jumps; in this case the data points are above the diagonal. The converse case, of orientational jumps occurring without a concomitant spectral jump, is not significant; they are either coincidental or due to analysis errors, e.g., an undetected spectral jump below the threshold criterion. In all trajectories together 1108 spectral jumps and 570 angular jumps were detected. For 86% of the angular jumps a spectral jump occurred simultaneously.

The distribution of the angular jump sizes is shown in Figure 7d. To understand the jump size distribution it is important to recall the structural organization of the M41S material. This system is characterized by hexagonally arranged unidimensional pores which form ordered domains of typically 100−200 nm in size. The domains are interconnected and randomly oriented with respect to each other. Furthermore, it is known that the structure also shows regions with curved and interrupted pores.

A complete rotation of the TDI molecules, which are about 2.5 nm long, in the 3−4 nm sized pore is most probably hindered by the presence of the CTAB template. Therefore, the distribution of angular jump sizes for a molecule in a pore is likely to be narrow. In contrast to this, the angular jumps are expected to be equally distributed for molecules moving between domains or in defects, since the relative orientation of neighboring domains are random and defect sites provide enough space for the molecule to freely rotate. The observed distribution shows the presence of at least two subpopulations of jump sizes. The first subpopulation corresponds to jumps below 30°, which are overrepresented. In this subpopulation only small angular jumps are allowed. This presumably reflects the influence of the geometric constraints in the pore on the orientational motion of the molecules. The second subpopulation is superimposed as an offset on the whole distribution (see line in Figure 7d). In this subpopulation the size of angular jumps are equally distributed. Most probably these jumps occur in regions between domains or at defect sites which are larger than the molecules dimensions.

Figure 7e displays the distribution of spectral jump sizes. Likewise, this distribution does not follow a monoexponential decay (note the logarithmic scale), indicating the presence of strong heterogeneities such as local changes, structural deformation, or impurities. The median is 7 nm and gives the characteristic amplitude of the spectral jumps. Furthermore, we investigated whether there is a correlation between magnitudes of spectral and orientational jumps. In Figure 7f we display the sizes of concomitant spectral versus angular jumps. No significant correlation is observed. The emission spectrum of the single molecules is determined by the chemical nature of the local environment which is spatially heterogeneous.

Therefore, a molecule moving within the mesoporous structure experiences different environments leading to different spectral jumps.

Comparison between Oxazine-1/$AlPO_4$-5 and TDI/M41S Systems. The two host−guest systems, oxazine-1 in $AlPO_4$-5 and TDI in M41S, show different types of spectral/orientational behaviors as expected from a comparison of guest and pore sizes. In the oxazine-1/$AlPO_4$-5 system, where the individual molecules are fixed, we observe spectral fluctuations of small amplitude (3−5 nm) and, rarely, pronounced spectral jumps of 10 nm and above. In $AlPO_4$-5 all molecules showed a distinct and stable orientation along the channel axis in accordance with what was reported in a previous study.[36] The spectral dynamics thus arise from extrinsic effects, which can be divided into rare distinct events (e.g., charge dislocation between strong adsorption sites in the vicinity of the molecule) and frequently occurring events (fluctuations of the host structure, diffusion of coadsorbed species) which lead to spectral diffusion. The molecule in this medium acts as a reporter on a particular location.

In contrast the TDI/M41S system provides more freedom for the mobility of the guests. The dynamic behavior is therefore more complex. First, in this host−guest system the molecules are found to switch between fixed orientations (adsorbed states) and undefined orientations (tumbling movement of the molecules) on different time scales, as the molecules move between adsorption sites in the material. Second, the emission spectra show fluctuations similar in magnitude to the ones found in the oxazine-1/$AlPO_4$-5 system. However, the frequency of the occurring jumps is (i) higher (3 spectral jumps >10 nm/min for TDI compared to 0.3/min for oxazine-1) and (ii) 86% of the observed orientational jumps occur simultaneously with a spectral jump. The spectral behavior in this sample is a superposition of (at least) two effects, namely uncorrelated spectral fluctuations (which were also observed in oxazine-1/$AlPO_4$-5) and spectral fluctuations arising from different environments explored by the mobile molecule. The molecule acts as an active reporter, exploring different environments.

Conclusion

The simultaneous examination of spectral and orientational behavior of a single guest molecule in a host material provides

valuable information for the characterization of the structural and chemical heterogeneities in the host. Moreover, the relative size of the guest molecule with respect to the pores of the host affects the observed dynamics. Oxazine-1 molecules tightly fit in the pores of the microporous $AlPO_4$-5. The resulting host/guest material represents a static material, i.e., rigid in nature, where the incorporated molecules are entrapped at a specific site in the host structure. In the second system studied the relevant sizes of the TDI molecules and the pores of the mesoporous M41S films allow for a slow mobility of the guest in the host pores. First, we observe that the typical motion of TDI molecules in the pores of M41S is not continuous but interrupted by stops at adsorption sites. Additionally, we find that in the TDI/M41S system the observed spectral dynamics are correlated with the orientational dynamics and thus arise directly from the different environments and adsorption sites that become explored by a mobile molecule.

Acknowledgment. We thank Klaus Müllen for providing the TDI dye molecule. This project was funded by the SFB 486.

JA0684850